# STATUS OF THE ILC CRAB CAVITY DEVELOPMENT

G. Burt, A. Dexter, Cockcroft Institute, Lancaster University,  LA1 4YR, UK
C. Beard, P. Goudket, P. McIntosh, ASTeC, STFC, Daresbury laboratories, WA4 4AD, UK
L. Bellantoni, Fermi National Accelerator Lab, Batavia IL   60510   U.S.A.
T. Grimm, Niowave, Inc, Lansing, MI 48906 USA
1.    Z. Li, L. Xiao, SLAC, Menlo Park, California

*Abstract*
The International Linear Collider (ILC) will require two dipole cavities to "crab" the electron and positron bunches prior to their collision. It is proposed to use two 9 cell SCRF dipole cavities operating at a frequency of 3.9 GHz, with a transverse gradient of 3.8MV/m in order to provide the required transverse kick. Extensive numerical modelling of this cavity and its couplers has been performed. Aluminium prototypes have been manufactured and tested to measure the RF properties of the cavity and couplers. In addition single cell niobium prototypes have been manufactured and tested in a vertical cryostat.

## INTRODUCTION

The International Collider (ILC) [1] collides bunches of electrons and positrons at a crossing angle of 14 mrad. The angle between these bunches causes a loss in luminosity due to geometric effects [2]. The luminosity lost from this geometric effect can be recovered by rotating the bunches into alignment prior to collision. One possible method of rotating the bunches is to use a crab cavity [3]. A crab cavity is a transverse defecting cavity, where the phase of the cavity is such that the head and tail of the bunch receive equal and opposite kicks. As the bunches are only 500 nm wide in the horizontal plane, the cavity phase must be strictly controlled to avoid the bunch centre being deflected too much. In order to keep the phase stability within the required limits it is required that the cavity be superconducting to avoid thermal effects in both the cavity and its RF source.

At the location of the crab cavity in the ILC there is only 23 cm separation between the centre of the cavity and the extraction line, hence the cavity must be small enough to fit in this space.  This, along with the difficulty of making high frequency SRF components, set the frequency of the cavity to 3.9 GHz.

## CAVITY SIMULATIONS

The cavity was required to operate at as high a gradient as possible to minimise longitudinal space. The iris radius, iris curvature and equator curvature were all altered and the electrical properties of the dipole mode were recorded. The equator radius was simultaneously altered in order to keep the resonant frequency at 3.9 GHz. The minimum iris radius was set at 15 mm due to the beam halo. The cavity shape was optimised in Microwave Studio [4] using a mesh of 40 lines per wavelength. In deflecting mode cavities there is generally a very high surface magnetic field at the iris, and comparably low surface electric fields. Hence the cavity was optimised to maximise the ratio of gradient to surface magnetic field. Figure 1 shows the variation in the voltage to surface magnetic field ratio as a function of iris radius.
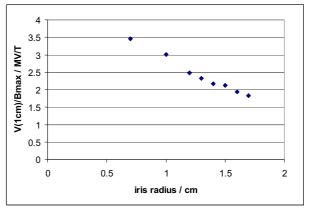


Figure 1. Optimisation of the ratio of accelerating gradient 10mm off axis and the surface magnetic field with varying iris radius.

The frequency spacing between the $\pi$ mode and the $8\pi/9$ mode was also maximised to enable the cavity to be accurately tuned for field flatness when warm. Other parameters observed were R/Q, geometry factor, and peak surface electric field. The optimised cavity shape is given in Figure 2 and 3 and the dimensions are given in Table 1.
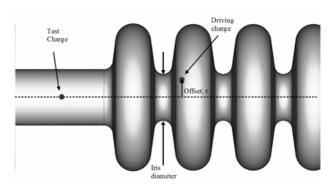


Figure 2 Schematic of the crab cavity geometry and illustrating the essential parameters (offsets not to scale)
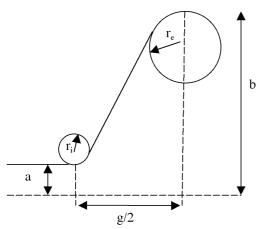
Figure 3: Cell Shape Parameters

Table 1: Cell Shape Parameters.

| | | mid-cell | trans-cup | End-cup |
|---|---|---|---|---|
| half cell length | g/2 | 19.2mm | 19.2mm | 18.6mm |
| iris radius | a | 15.0mm | 15.0mm | 18.0mm |
| iris curvature | $r_i$ | 5.5mm | 5.5mm | 5.5mm |
| equator radius | b | 47.18mm | 47.37mm | 47.37mm |
| equator curvature | $r_e$ | 11.41mm | 11.41mm | 11.41mm |

Table 2: Crab Cavity Eigenmode Simulation Results for Dipole Modes.

| Frequency (GHz) | Phase Advance (degrees) | (R/Q)' (Ohms) |
|---|---|---|
| 3.908 | 180 | 235.40 |
| 7.082 | 160 | 2.33 |
| 7.136 | 180 | 6.55 |
| 7.178 | 180 | 3.62 |
| 7.390 | 160 | 2.03 |
| 8.039 | 20 | 4.31 |
| 10.029 | 120 | 1.13 |
| 10.054 | 140 | 0.73 |
| 12.980 | 140 | 0.53 |
| 12.996 | 120 | 1.08 |
| 13.014 | 100 | 0.45 |
| 17.550 | 120 | 0.15 |
| 17.561 | 100 | 0.30 |

In order to maximise the cavity packing factor, and hence reduce longitudinal space, a multi-cell cavity was chosen. This mean that the crab cavities on each beamline could be placed closer to each other, simplifying the phase control problem. It was decided that a nine cell cavity would be achievable in terms of mode spacing and wakefields.

The frequencies and R/Q's of the nine cell cavity were calculated in the 2D eigensolver of the computer code MAFIA [5]. A mesh of 350,000 elements was used for the final simulations after checking the modal convergence as the mesh was increased. All dipole modes up to 18.5 GHz and all TM-like monopole modes up to 16 GHz were calculated [6].

The cavity was given 150 mm beam-pipes to ensure that the fields of all trapped or non-propagating modes were sufficiently attenuated by the ends of the beam-pipes. The simulation results for the dipole modes are shown in Figure 4.
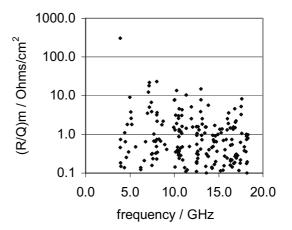


Figure 4. Crab Cavity Eigenmode Simulation Results for Dipole Modes.

The solver was run first with perfect electrical conductor boundaries at the end of the beampipe, and were then repeated with perfect magnetic conductor boundaries. The frequencies calculated for each mode were compared to show which modes had large fields at the end of the beam-pipes. It was found that for that for the 1st monopole passband (known as the lower order mode, LOM) and for the 13 dipole modes with the highest R/Q's (shown in Table 2) the frequency change when altering the boundaries was less than 1%.

It was found that the highest monopole R/Q's were that of the LOM and the highest dipole R/Q was due to the operating mode and it's opposite polarisation.

## NORMAL CONDUCTING PROTOTYPE MEASUREMENTS

In order to verify the simulations, a normal conducting prototype of the cavity was constructed from aluminium. The cavity was made in a modular set-up so different numbers of cells could be analysed. For the higher frequency modes a reflectometry measurement was used by sending a oscillating signal down a wire stretched along the cavity [7]. The dominant mode of a coaxial wire stretched centred in a cavity is TEM in nature. As the fields excited are similar to those of an ultra-relativistic beam in free space then any fields scattered from discontinuities (irises in our case) will represent the wake-field. Thus, we "simulate" a charged particle beam with a wire stretched through the cavity. However the presence of the wire will strongly perturb modes with a strong longitudinal electric field near the wire, such as monopole modes. If the wire is slightly off-axis the wire will couple to the dipole modes of the cavity without significantly perturbing them. The impedance for the 1st dipole passband as a function of wire offset is shown in Figure 5.

The scattering matrix of the cavity and wire was measured using a network analyser. A linearly tapered beam-pipe was used to alter the beam-pipe size from 7 mm to 18 mm with minimal mode scattering. The measurements were taken with the wire on and off axis in order to find the transmission of the system with and without dipole mode coupling.
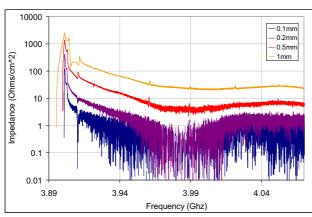
Figure 5. Impedance of the 1st dipole passband for various wire offsets.

It was found that the frequency and R/Q of the modes varied at larger offsets due to the perturbation of the wire hence most measurements were taken at small offsets. The measurements were repeated several times in order to evaluate the effect of temperature, cable movements and the sensitivity to cavity alignment. As the cavity was modular small misalignments between the cavities were possible during any movement of the cavity, this was found to cause a large spread in the measurements. This is likely to be a good indication of the sensitivity to manufacturing defects.
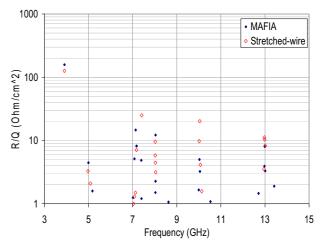
Figure 6. Comparison of measured and simulated R/Qs for a 9 cell crab cavity.

The measurements were able to calculate the frequency and R/Q of most of the 11 most significant dipole modes as identified from MAFIA up to a frequency of 13.1 GHz. Two of the modes around 7 GHz were unable to be identified as the wire coupled strongly to a passband of monopole modes at that frequency. The R/Q's measured are compared to the MAFIA simulations in Figure 6.

Bead-pull measurements are now underway to measure the field profile of the modes below the beam-pipe cut-offs.

## COUPLER DESIGN AND TESTING

The computer code Omega3P [8] was used to investigate the effectiveness of the couplers designed for the FNAL deflecting mode cavity. The original FNAL design for the couplers had three problems associated with it

1) There was coupling between two modes of opposite polarisation in the 1st dipole passband due to the transverse squashing of the cavity.
2) The HOM/LOM coupler notch filters were very sensitive to small changes.
3) The damping of the SOM was not sufficient for the ILC requirements.

The mode coupling was reduced by increasing the frequency separation between the two polarisations. This was achieved by increasing the squashing the cavity transversely until the frequency separation between the two polarisations is 15 MHz.

The HOM coupler is a shorted coaxial structure with the RF removed through a coupling antenna similar to the FNAL 3rd harmonic HOM coupler [9].

The HOM coupler was redesigned with a less sensitive filter. The notch filter is much less sensitive to small changes when the capacitive gap is much larger, hence the gap was increased to 3.1 mm and the length of the inner conductor was adjusted accordingly to keep the filter at 3.9 GHz. This improved the sensitivity from 1.6 MHz/μm to 0.1 MHz/μm. The 2nd stub was also

straightened to remove a multipactor problem, which removed the magnetic loop coupling.

The LOM coupler was very similar to the HOM coupler except that the tip of the probe hooks round into the cavity. The notch filter was removed from the LOM coupler by moving it opposite the SOM coupler. At this location the LOM coupler, like the SOM coupler, does not couple to the operating mode as it is positioned at a field null. This meant that the can didn't require the short and the coupling antenna and the coaxial line continues to the HOM load. In addition, to simplify the design this design only requires a single stub.
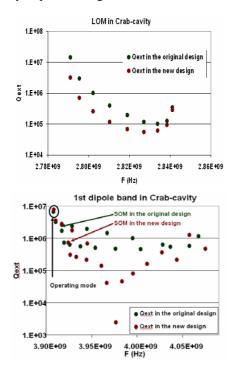


Figure 7.  External Q for the 1st two passbands in the crab cavity.

The SOM coupler is a simple coaxial line with the inner conductor penetrating into the beam-pipe. The damping of the SOM was increased by increasing the size and penetration of the coupler to make it similar to the input coupler. A copper model of this coupler was manufactured and tested on the normal conducting prototype cavity. The measured external Q was found to agree with the simulations performed on Microwave Studio [X].
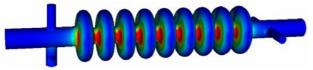


Figure 8. The SOM in the ILC crab cavity

Currently work is underway to combine the SOM and LOM couplers in order to reduce the number of couplers required.

The current design of the cavity and couplers is shown in Figure 8. Simulations of this structure were performed in Omega-3P to determine the external Q factors of the 1st three cavity passbands [10], results shown in Figure 7. Copper models of the HOM and LOM couplers are currently being manufactured and will be used to measure the external Q of some of the modes in the cavity.

Multipacting in the cell and LOM/HOM couplers are simulated using Track3P. No multipacting activities have been found in the cell and LOM coupler up to a peak transverse field gradient of 5MV/m. We do find resonant particle trajectories in the HOM pickup region. The impact energies of the electrons are between 85 eV and 240 eV, and this energy range is too low to cause multipacting for the copper pickup probe. Preliminary studies show that by rounding the pickup shape with curved surface, the occurrences of resonant trajectories can be reduced.

## SINGLE CELL PROTOTYPE SRF TESTS

Three single cell niobium prototypes of the crab cavity have been manufactured by Niowave for preliminary tests, shown in Figure 9. Two of these cavities have been tested at a temperature of 1.8K. The ohmic Q factor of the cavity was measured as the cavity was cooled down from 4.2K to 1.8 K.



Figure 9. A single cell crab cavity read for insertion into the vertical cryostat

Using MWS calculations of the Geometry factor of the cavity we were able to calculate the resistance of the surface as we cooled down. By fitting the curve to the BCS resistance we were able to estimate that a residual resistance of 600 n$\Omega$ was achieved in both cavities, shown in Figure 10. This was much higher than expected. However as the mode measured is a dipole mode it will couple to the TE11 mode of the beam-pipe and will penetrate further than monopole modes. Further MWS simulations showed that the fields were able to penetrate to the stainless steel flange 80 mm down the beam-pipe. It is suspected that the high residual resistance values were

due to this stainless steel beam-pipe. The cavity reached a the design gradient of 6 MV/m without quench. Previous tests at FNAL on 3 cell deflecting mode cavities at 3.9 GHz, on which the crab cavity is based, achieved a residual resistance of 39±7 nΩ.
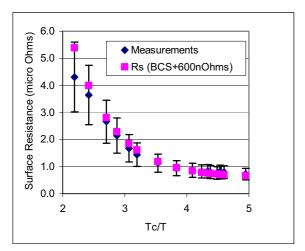


Figure 10. Surface resistance against temperature for 1st the single cell test.

In order to reach the expected surface resistance we plan to replace the copper conflat gaskets with niobium discs with holes big enough for the couplers. This would eliminate losses except at the NbTi, the NbTi-Nb mechanical joint and the copper antennas. The niobium gasket would make the vacuum seal, the rf mechanical joint and carry the rf currents on the superconducting surface, thereby shielding the current from the stainless steel. This method has worked with some success at Fermilab.

## CONCLUSION

A first order design of the ILC crab cavity and its couplers is complete and a copper prototype of the full system is currently being manufactured. In addition two single cell SRF cavities have been manufactures, processed and tested. In these cavities the design gradient has been reached, although with a lower Q than expected.

In the next phase we plan to complete the testing of the copper prototype and to start construction of a full SRF prototype of this cavity.

## REFERENCES

[1] International linear Collider Reference Design Report (Feb 2007), [online] http://media.linearcollider.org/rdr_draft_v1.pdf
[2] G. Burt, Effect and tolerances of RF phase and amplitude errors in the ILC crab cavity, EUROTeV-Report-2006-098, 2006
[3] R. B. Palmer, Energy scaling, crab crossing and the pair problem SLAC-PUB-4707, 1988
[4] Microwave Studio, CST GmbH, Darmstadt, 1994 [online] http://www.cst.com/.
[5] The MAFIA Collaboration, CST GmbH, Darmstadt, 1994 [online] http://www.cst.com/.
[6] G. Burt, Analysis of Damping Requirements for Dipole Wake-Fields in RF Crab Cavities, Vol 54, Issue 5, Part 2 of TNS (October 2007)
[7] P. Goudket, Impedance Measurements on a Test Bench Model of the ILC Crab Cavity , WEPMN077, PAC 2007, Albuquerque, US
[8] Omega 3P, SLAC, Palo Alto, US
[9] N.Solyak, high field test results of superconducting 3.9 GHz accelerating cavities at FNAL, THP061, Linac 2006, Knoxville, US.
[10] L. Xiao, HOM and LOM coupler optimisation for the ILC crab cavity, WEPM050, PAC 2007, Albuquerque, US